PUBLICATIONS OF THE ASTRONOMICAL SOCIETY OF THE PACIFIC, **113**:66–71, 2001 January

Passbands and Theoretical Colors for the Washington System

MICHAEL S. BESSELL

Research School of Astronomy and Astrophysics, Institute of Advanced Studies, The Australian National University, Cotter Road, ACT 2611, Australia; bessell@mso.anu.edu.au

Received 2000 July 10; accepted 2000 September 21

ABSTRACT. The passbands of the Washington system (C, M, T_1, T_2) have been checked through synthetic photometry of the Vilnius spectra and comparison of observed and synthetic color-color relations. Using the derived passbands, theoretical colors were computed using the grid of ATLAS no-overshoot models of Castelli. These can be used for calibration of the Washington system.

1. INTRODUCTION

The broadband Washington system of photometric standards was established by Canterna (1976) and Geisler (1990). The Washington system was devised to use the wideband sensitivity of GaAs phototubes and CCDs and makes use of the sensitivity of blue-violet colors to metallicity and gathers more violet light in cool stars. Most of its colors can be well transformed into related colors in the Cousins *BVRI* system; some transformations were given in Bessell (1992). An empirical abundance calibration was originally provided by Geisler (1986), and a revised calibration of the system was given by Geisler, Claria, & Minniti (1991). Theoretical colors based on new model atmospheres would be a very useful supplement to the empirical calibrations of the Washington system which is now being used for wide-field surveys of the abundances and distribution of stars.

In this paper we first describe checks made of the passbands of the Washington system using the Vilnius Spectrophotometric Atlas (Straizys & Sviderskiene 1972). Then using the finally adopted passbands, we computed theoretical colors from the ATLAS no-overshoot model fluxes that were used to synthesize colors in the *UBVRIJHKL* system by Bessell, Castelli, & Plez (1998), Castelli (1999), and Bessell & Castelli (2000). Finally, we compare the theoretical $C-M$ versus $M-T_2$ colors for theoretical isochrone giant branches with observations of giant stars covering a wide range of metallicity.

2. PASSBANDS AND COMPARISONS WITH OBSERVATIONS

2.1. Washington System Passbands

Relative response functions were given for the Washington system by Canterna (1979). We began by modifying these passbands to account for photon-counting observations.

The number of photons counted in passband R_X for a star with flux $f(\lambda)$ is given by

$$\int [f(\lambda)/h\nu]R_X(\lambda)d\lambda = (1/hc)\int f(\lambda)[\lambda R_X(\lambda)]d\lambda.$$

This rearrangement shows how one can use the same fluxes with the $\lambda R_X(\lambda)$ responses to compute synthetic photon counting photometry. The relative response functions of Canterna were therefore multiplied by the wavelength and renormalized to generate λR_X passbands relevant for photon-counting detectors such as CCDs (see, e.g., Bessell & Germany 1999).

Synthetic photometry of the Vilnius spectra was made for the C, M, T_1, T_2, V, and I bands. From these calculations, the effective wavelengths of the synthetic Washington system passbands relative to the standard V band were assessed by comparing observed and computed regressions between $C-V$, $M-V$, $V-T_1$, and $V-T_2$ versus $V-I$. Linear fits to $V-I$ were made for the observations and for the synthetic photometry. These are discussed in detail below. The observed data were restricted to those stars with near-solar metallicities and with $V-I$ colors bluer than $V-I = 1.7$. For the Vilnius spectra, the comparison was restricted to luminosity class V and III spectra and the same color range.

The coefficients of the linear fits to the synthetic and observed colors were not identical, indicating that the initially adopted passbands did not reproduce the true passbands exactly. However, it was still possible to bring the coefficients into agreement either by scaling the synthetic colors or by slightly shifting the passbands. Scaling colors is the equivalent of the derivation of slopes or color terms in normal standardized photometry.

The scaling factors were 1.04, 0.91, 1.02, and 1.02 for $C-V$, $M-V$, $V-T_1$, and $V-T_2$, respectively. Such scaling factors were found computationally to be equivalent to shifting the photon-counting passbands for C, M, T_1, and T_2 by about -5, $+3.7$, $+3$, and $+9$ nm, respectively. Either way of accounting for

TABLE 1
NORMALIZED $\lambda R_X(\lambda)$ RESPONSES

λ	C	λ	M	λ	T_1	λ	T_2
300	0.000	430	0.000	560	0.000	720	0.000
310	0.030	440	0.015	570	0.037	730	0.130
320	0.157	450	0.158	580	0.103	740	0.540
330	0.364	460	0.448	590	0.197	750	0.698
340	0.591	470	0.708	600	0.663	760	0.803
350	0.762	480	0.866	610	0.968	770	0.875
360	0.860	490	0.950	620	1.011	780	0.911
370	0.935	500	0.993	630	0.937	790	0.932
380	0.984	510	0.996	640	0.842	800	0.954
390	1.004	520	0.944	650	0.744	810	0.975
400	0.987	530	0.886	660	0.656	820	0.987
410	0.920	540	0.800	670	0.556	830	0.999
420	0.819	550	0.682	680	0.448	840	0.999
430	0.682	560	0.518	690	0.359	850	0.979
440	0.542	570	0.339	700	0.291	860	0.945
450	0.366	580	0.190	710	0.241	870	0.844
460	0.168	590	0.084	720	0.164	880	0.620
470	0.049	600	0.016	730	0.118	890	0.000
480	0.000	610	0.000	740	0.069		
				750	0.042		
				760	0.024		
				770	0.000		

the small mismatch between the observed and computed bands is acceptable and well within the observational errors, but for computational simplicity we decided to shift the bands.

Table 1 lists the finally adopted λR_X passbands for C, M, T_1, and T_2; the V and I passbands are given in Bessell (1990). In Figure 1 are shown the CMT_1T_2 passbands together with those for the *UBVRI* system.

2.2. Standard Stars and Vilnius Spectra

In Table 2 are listed CMT_1T_2 photometry for some of the Geisler (1990) standard stars which have *BVRI* photometry. The sources of the *BVRI* photometry are indicated. These data were used to derive the relations in Bessell (1992) and are the source of the observational data used in this paper.

The linear fits between $V-T_1$, $V-T_2$, and $V-I$ were excellent while that for $M-V$ was well defined, although systematic nonlinear deviations were evident. The regression between $C-V$ and $V-I$, which is similar to that between $U-B$ and $B-V$, was more problematic for two reasons. First, large nonlinearities were present; second, for the cooler stars (spectral types later than F5), the $C-V$ value is sensitive not only to temperature but also to luminosity class, which is not well known for many of the random field stars used as standards. As a result, the match between the observed and computed $C-V$ versus $V-I$ regression is not as well restrained as for the other colors.

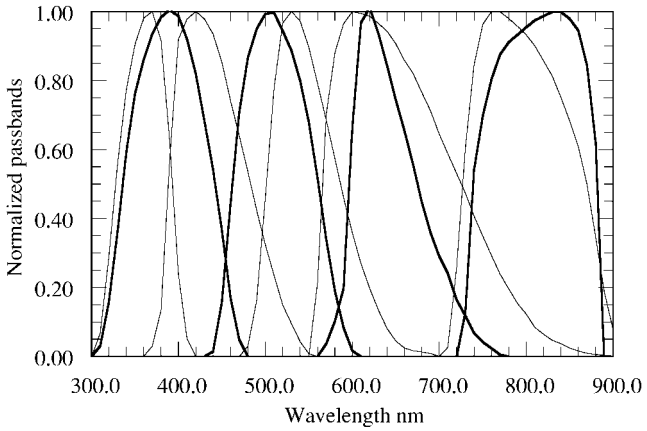

FIG. 1.—Adopted $\lambda R(\lambda)$ response for C, M, T_1, and T_2 (*thicker lines*) compared to the standard *UBVRI* passbands (*thin lines*).

The formal linear fits to the observations were as follows:

$$C - V = -0.201 + 1.55(V - I),$$

$$M - V = 0.006 + 0.25(V - I),$$

$$V - T_1 = -0.007 + 0.51(V - I),$$

$$V - T_2 = -0.009 + 1.018(V - I).$$

Figures 2–5, respectively, show the residuals to the linear fits to the observed $C-V$, $M-V$, $V-T_1$, and $V-T_2$ versus $V-I$ regressions together with residuals to the synthetic colors derived from the Vilnius spectra using the adopted passbands of Table 1. The synthetic colors are seen to be in good agreement with the observations.

3. MODEL ATMOSPHERE COLORS

3.1. Electronic Tables of Colors

The grid of model atmosphere fluxes computed by Castelli (1999) were used to produce the theoretical colors in this paper. The solar abundance models and *UBVRIJHKL* colors were discussed by Bessell et al. (1998). Castelli (1999) discussed the model computational details and the other abundance models. Table 3 identifies the tables containing the theoretical colors corresponding to the different abundances.[1]

The reliability of the theoretical fluxes and their relevance for temperature derivation are discussed in Bessell et al. (1998), where the agreement between the theoretical *UBVRIJHKL* colors and observations for the solar composition grid is reviewed and where comparison between fundamental temperatures and model temperature versus $V-I$ is made. Castelli (1999) discusses theoretical *UBV* colors for the whole grid of different

[1] These tables are available electronically from http://www.mso.anu.edu.au/~bessell/FTP/Washington.

TABLE 2
STARS WITH COMMON PHOTOMETRY

Star	T_1	$C-M$	$M-T_1$	T_1-T_2	V	$B-V$	$V-R$	$V-I$	Observer
HD 2796	8.042	0.652	0.672	0.508	8.500	0.730	0.481	0.967	B
HD 4306	8.575	0.579	0.656	0.502	9.010	0.737	0.449	0.922	B
CD −38°245	11.480	0.678	0.723	0.541	11.980	0.800	0.502	1.010	B
HD 4965	7.190	0.106	0.086	0.068	7.256	0.113	0.065	0.125	C1, C2
092−342	11.359	0.331	0.380	0.290	11.622	0.448	0.263	0.543	M, L2
092−263	11.260	1.249	0.811	0.538	11.774	1.067	0.531	1.060	M, L2
CD −30°298	10.396	0.431	0.599	0.466	10.780	0.635	0.405	0.847	B
HD 16581	8.235	−0.212	−0.047	−0.036	8.192	−0.068	−0.024	−0.054	M, C1, J
HD 16608	7.552	1.931	1.164	0.795	8.331	1.506	0.807	1.554	C1, J
CD −24°1782	9.525	0.448	0.590	0.448	9.910	0.626	0.401	0.828	B
BD +6°648	8.366	1.390	1.043	0.736	9.100	1.320	0.749	1.486	B
HD 29574	7.606	1.597	1.145	0.786	8.340	1.406	0.774	1.506	B
096−737	11.009	1.553	1.060	0.742	11.711	1.335	0.720	1.418	M, L2
096−406	9.188	0.200	0.173	0.125	9.302	0.218	0.118	0.243	M, L2
HD 40983	8.564	−0.060	0.003	0.007	8.553	0.007	0.006	0.010	C1, J
HD 41029	7.687	1.146	0.747	0.484	8.180	0.979	0.513	0.978	C1, J
098−185	10.430	0.166	0.155	0.123	10.539	0.194	0.112	0.237	M, L2
098−193	9.454	1.447	0.893	0.570	10.044	1.177	0.605	1.139	M, L2
098−650	12.223	0.117	0.117	0.096	12.271	0.153	0.079	0.165	L2
098−A	12.395	2.306	1.532	1.101	13.420	1.950	1.084	2.075	B
098−670	11.242	1.642	1.050	0.696	11.930	1.362	0.716	1.369	L2
098−676	12.426	1.226	0.975	0.724	13.068	1.159	0.676	1.346	L2
098−682	13.426	0.580	0.522	0.345	13.749	0.641	0.361	0.712	L2
098−685	11.694	0.393	0.407	0.297	11.954	0.467	0.286	0.566	L2
098−320	8.633	1.420	0.870	0.553	9.199	1.162	0.584	1.107	M, L2, J
098−334	10.266	−0.005	0.049	0.052	10.290	0.056	0.035	0.077	J
HD 63368	7.938	1.042	0.736	0.510	8.430	0.944	0.514	0.999	C1, J
HD 63390	8.745	0.035	0.021	0.019	8.740	0.053	0.003	0.017	C1, J
HD 84916	8.100	1.430	0.871	0.551	8.678	1.159	0.591	1.123	C1, J
HD 84971	8.722	−0.515	−0.094	−0.086	8.642	−0.155	−0.059	−0.142	M, C1, J
102−466	8.723	1.273	0.820	0.525	9.256	1.075	0.554	1.061	M, L2
102−472	8.250	1.205	0.768	0.504	8.760	1.030	0.523	1.000	M, L2
102−58	9.357	0.028	0.053	0.017	9.377	0.063	0.039	0.053	M, J, L2
HD 97991	7.506	−0.668	−0.152	−0.133	7.394	−0.224	−0.094	−0.229	C1, C2, J
HD 98007	8.545	0.757	0.577	0.370	8.940	0.729	0.393	0.750	C1, J
M3680−10	12.580	0.351	0.393	0.281	12.840	0.437	0.260	0.532	B
M3680−27	10.190	1.386	0.865	0.563	10.775	1.147	0.599	1.132	B
M3680−6	12.168	0.437	0.451	0.313	12.477	0.508	0.310	0.606	B
HD 104893	8.574	1.348	0.992	0.680	9.240	1.232	0.688	1.331	B
104−461	9.435	0.363	0.416	0.298	9.706	0.484	0.285	0.571	M, L2
HD 118129	7.642	1.299	0.802	0.506	8.188	1.076	0.543	1.029	C1
HD 118246	8.107	−0.432	−0.070	−0.047	8.040	−0.154	−0.050	−0.111	M, C1, J, L2
HD 122563	5.656	0.875	0.787	0.571	6.196	0.912	0.550	1.095	C1, C2
BD +1°2916	8.919	1.543	1.045	0.702	9.600	1.350	0.717	1.402	B
HD 126587	8.615	0.706	0.731	0.548	9.120	0.827	0.504	1.044	B
HD 148816	6.970	0.411	0.472	0.344	7.286	0.546	0.320	0.647	C1, C2
HD 157881	6.700	1.620	1.197	0.818	7.514	1.378	0.845	1.605	M, C1, C2
HD 161261	8.246	−0.084	0.066	0.037	8.279	0.044	0.046	0.079	C1, J
HD 171731	8.468	1.362	0.883	0.554	9.085	1.134	0.619	1.175	C1, J
HD 171732	8.945	0.125	0.264	0.208	9.122	0.274	0.187	0.391	C1, J
110−499	11.182	0.970	0.871	0.721	11.737	1.001	0.593	1.267	L2
110−502	11.074	2.722	1.905	1.403	12.330	2.245	1.382	2.629	L2
110−503	11.434	0.674	0.550	0.462	11.773	0.681	0.368	0.802	L2
110−506	11.013	0.489	0.476	0.334	11.312	0.575	0.331	0.647	L2
110−507	11.850	1.294	0.919	0.617	12.440	1.154	0.626	1.200	L2
HD 184266	7.230	0.457	0.539	0.403	7.600	0.575	0.370	0.776	B
HD 184711	7.248	1.446	1.098	0.768	7.980	1.326	0.742	1.482	B
HD 205584	7.090	1.579	0.935	0.587	7.705	1.254	0.626	1.186	M, C1, J
HD 205556	8.342	−0.250	−0.038	−0.030	8.301	−0.061	−0.020	−0.060	C1, J
114−750	11.891	−0.222	0.016	−0.026	11.910	−0.045	0.025	0.008	M, L2
114−670	10.475	1.486	0.944	0.596	11.101	1.218	0.638	1.202	M, L2

[a] B: Bessell unpublished; C1, C2: Cousins 1984a, 1984b; J: Jones 1990, private communication; L1, L2: Landolt 1973, 1992; M: Menzies et al. 1991.

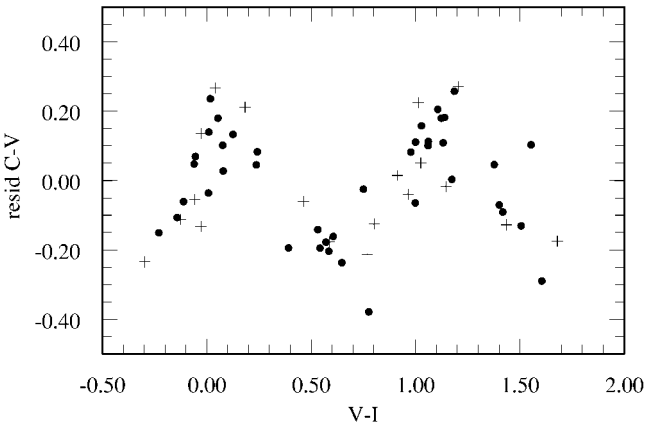

FIG. 2.—Residuals to $C-V$ vs. $V-I$ fit. Observations (*dots*) and synthetic photometry from Vilnius spectra (*plus signs*).

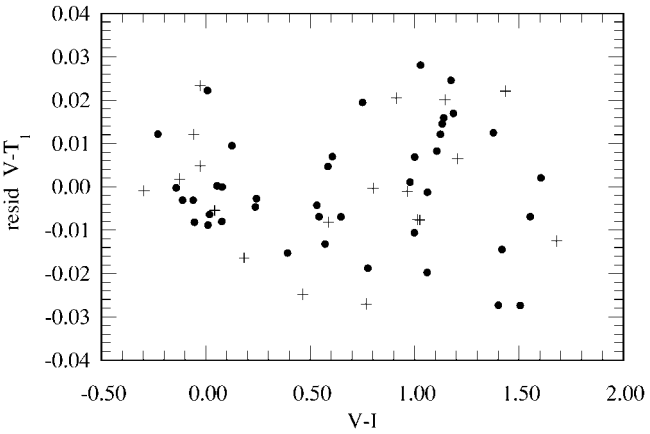

FIG. 4.—Residuals to $V-T_1$ vs. $V-I$ fit. Symbols as in Fig. 2.

metallicities. We believe that the theoretical colors from the no-overshoot models are good representations of the observed colors and good predictors of the temperatures and abundances of stars. Theoretical colors are particularly valuable for providing insight into the behavior of color-temperature and differential color-abundance relations for different abundances and effective gravities for which observations are sparse.

However, because of uncertainties in one-dimensional model atmospheres, uncertainties in line opacities, and uncertainties in adopted passbands, it is unlikely that exact agreement between observed and theoretical color-color, color-temperature, and differential color-metallicity relations exists. It is therefore best to use the theoretical colors to interpolate between data for stars with precisely determined colors, temperatures, and abundances or to use such data to calibrate the theoretical colors.

3.2. Theoretical Isochrone Colors and Comparison with Observations

In order to better compare theoretical colors with observations, it is necessary to produce colors for the temperatures and gravities relevant to giant branches. In Figure 6 are shown the schematic isochrone temperatures and gravities derived from Bertelli et al. (1994). The logarithmic ages selected for the isochrones were 9.5, 10.0, 10.08, 10.08, 10.08, and 10.08, respectively, for $[Fe/H]_{\odot} = 0.0, +0.4, -0.4, -0.7, -1.3$, and -1.7. Colors were interpolated from the grids at 250 K intervals in temperature between 5750 and 4000 K.

In Figure 7 is shown the relation between $T_{\rm eff}$ and $M-T_2$. Because of the long-wavelength baseline, $M-T_2$ is often used to derive temperature. It is clear that $M-T_2$ is a good temperature index with only a slight abundance sensitivity for solar and lower abundance stars. However, it is very sensitive to

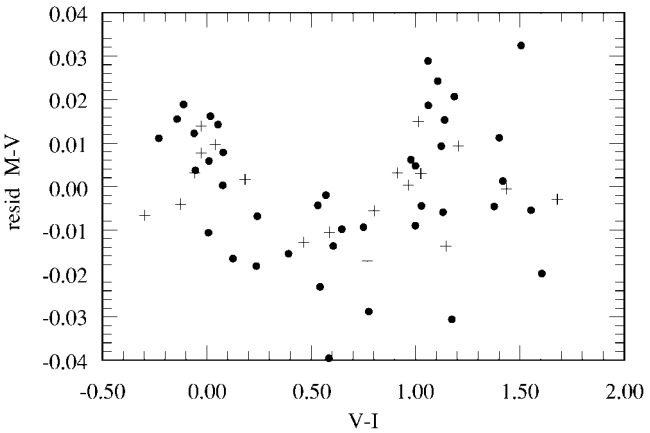

FIG. 3.—Residuals to $M-V$ vs. $V-I$ fit. Symbols as in Fig. 2.

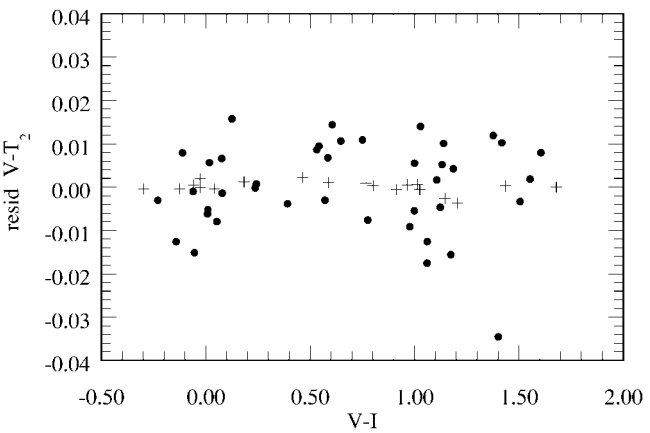

FIG. 5.—Residuals to $V-T_2$ vs. $V-I$ fit. Symbols as in Fig. 2.

TABLE 3
ELECTRONIC TABLES OF THEORETICAL COLORS

Table Number	[M/H]	[α/Fe]	Microturbulent Velocity (km s^{-1})
4	+0.5	0.0	2
5	0.0	0.0	2
6	−0.5	0.0	2
7	−1.0	0.4	1
8	−1.5	0.4	1
9	−2.0	0.4	1

effective gravity, as seen by the extreme red colors of the lowest gravity and lowest abundance models.

In Figure 8 are plotted the theoretical $C-M$ versus $M-T_2$ giant branch loci for different abundances. These are shown in comparison with observations. The mean cluster points are from Geisler et al. (1991), and the individual halo giants are listed in Table 2 and are taken from Geisler (1986). The individual stars have been dereddened by the $E(B-V)$ reddenings listed in that paper. The agreement between the theoretical loci and the observations is good except possibly for the reddest stars. As the $C-M$ color is very sensitive to gravity at low temperature, the rough interpolation between isochrones of different abundance may be partially responsible for the poorer fit at the red end. The coolest ATLAS models may also be somewhat uncertain. At the hotter end, the globular cluster points fit well, although the individual halo giants show some scatter. Perhaps some of the reddenings are overestimated.

4. CONCLUSIONS

The Vilnius spectra were used to check the passbands of the Washington system by computing synthetic colors and comparing them with observations. As a result, all the bands were moved slightly. Using these adopted passbands, theoretical colors in the Washington system were then computed for the grids of ATLAS9 no-overshoot model atmospheres computed by Castelli. Tables of the computed colors are available electronically. The theoretical calibration of the $C-M$ versus $M-T_2$ diagram was shown to agree very favorably with the empirical calibration. We believe that all the theoretical colors can be used for deriving reasonable temperatures and abundances but

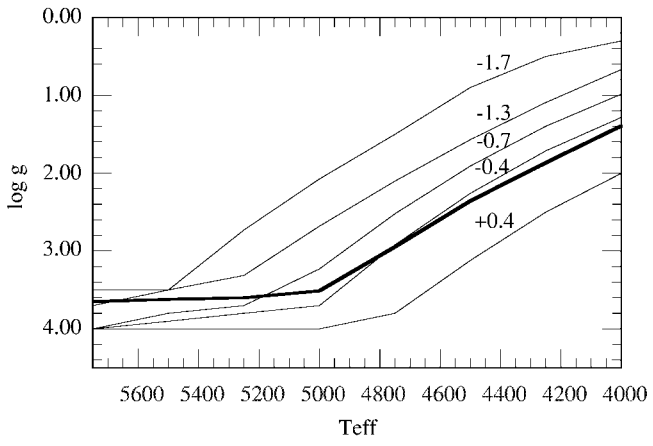

FIG. 6.—Schematic isochrone-derived giant branches. The thick line is the solar composition isochrone.

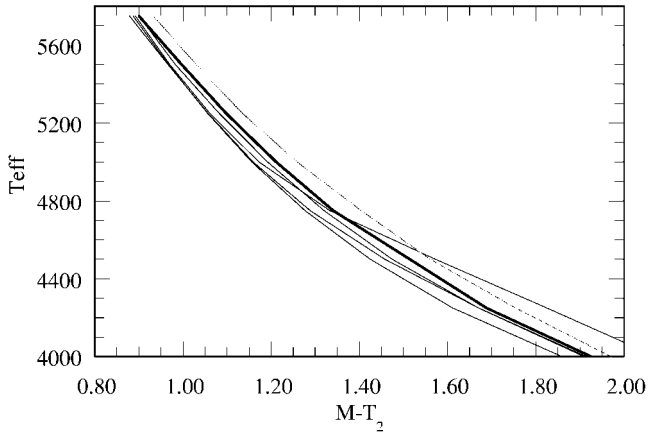

FIG. 7.—Theoretical $T_{\rm eff}$ vs. $M-T_2$ relation for abundances between $[{\rm Fe/H}]_\odot = +0.4$ and -2.0. The thick line is the solar composition locus. The upper dotted line is for $[{\rm Fe/H}]_\odot = +0.4$. The upper line at the bottom right is for the lowest abundance isochrone.

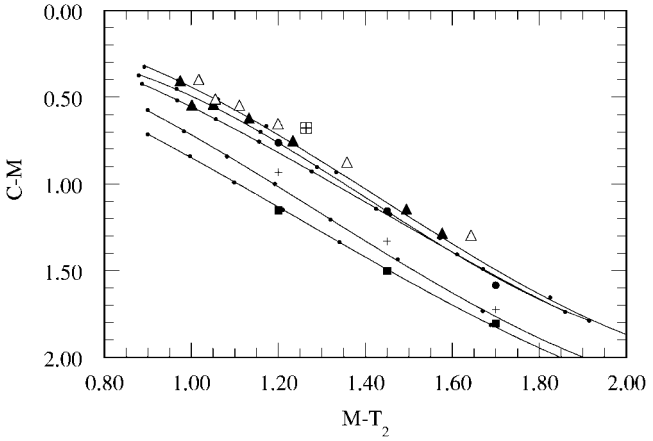

FIG. 8.—Theoretical $C-M$ vs. $M-T_2$ loci abundances for ($[{\rm Fe/H}]_\odot = 0.0$, -0.5, -1.0, -1.5, -2.0. The dots on the loci indicate the temperature grid points between $T_{\rm eff} = 5750$ and 4000 K. Mean cluster observations are given for solar composition (*filled squares*), NGC 104 ($[{\rm Fe/H}]_\odot = -0.8$; *plus sign*), and NGC 6752 ($[{\rm Fe/H}]_\odot = -1.5$; *filled circle*). The filled and open triangles are for individual bright halo field giants with abundances between -2.0 and -2.3 dex and between -2.3 and -3.0 dex, respectively. The crossed open square represents a star with an abundance of -4.0 dex.

urge additional empirical data be obtained so that the theoretical data can be used for interpolation rather than extrapolation.

I would like to thank Fiorella Castelli for use of her model atmospheres and for many discussions. I would also like to thank the referee Ron Canterna for his useful comments and John Norris for stimulating my renewed interest in the Washington system.

REFERENCES

Bertelli, G., Bressan, A., Chiosi, C., Fagotto, F., & Nasi, E. 1994, A&AS, 106, 275
Bessell, M. S. 1990, PASP, 102, 1181
———. 1992, in IAU Colloq. 136, Stellar Photometry—Current Techniques and Future Developments, ed. C. J. Butler & I. Elliott (Cambridge: Cambridge Univ. Press), 22
Bessell, M. S., & Castelli, F. 2000, A&A, in preparation
Bessell, M. S., Castelli, F., & Plez, B. 1998, A&A, 333, 231
Bessell, M. S., & Germany, L. 1999, PASP, 111, 1421
Canterna, R. 1976, AJ, 81, 228
———. 1979, in Dudley Observatory Report 14, ed. A. G. Davis Philip (Albany: Dudley Obs.), 489
Castelli, F. 1999, A&A, 346, 564
Cousins, A. W. J. 1984a, South Africa Astron. Obs. Circ., 8, 59
———. 1984b, South Africa Astron. Obs. Circ. 8, 69
Geisler, D. 1986, PASP, 98, 762
———. 1990, PASP, 102, 344
Geisler, D., Claria, J. J., & Minniti, D. 1991, AJ, 102, 1836
Landolt, A. U. 1973, AJ, 78, 959
———. 1992, AJ, 104, 340
Menzies, J. W., Marang, F., Laing, J. D., Coulson, I. M., & Engelbrecht, C. A. 1991, MNRAS, 248, 642
Straizys, V., & Sviderskiene, Z. 1972, Astron. Obs. Bull. Vilnius 35